IECMS 2018

sciforum

Conference Proceedings Paper

Oscillatory Zoned Gersdorffite and the Ni-Bi-Au Association at Clemence Mine and Km 3 Locality, Lavrion District, Greece

Emmanouil Galanos [1,*], Panagiotis Voudouris [1,*], Branko Rieck [2], Uwe Kolitsch [2,3], Constantinos Mavrogonatos [1], Vasilios Melfos [4], Stefanos Zaimis [5] and Konstantinos Soukis [6]

[1] Department of Mineralogy and Petrology, Faculty of Geology & Geoenvironment, National and Kapodistrian University of Athens, Athens, Greece; kmavrogon@geol.uoa.gr
[2] Institut für Mineralogie und Kristallographie, Universität Wien, Austria; rieckb49@univie.ac.at (B.R.); uwe.kolitsch@NHM-WIEN.AC.AT (U.K.)
[3] Mineralogisch-Petrographische Abteilung, Naturhistorisches Museum, Wien, Austria
[4] Department of Mineralogy-Petrology-Economic Geology, Faculty of Geology, Aristotle University of Thessaloniki, Thessaloniki, Greece; melfosv@geo.auth.gr
[5] Institut für Mineralogie, TU Bergakademie Freiberg, Freiberg, Germany; szaimis@gmail.com
[6] Department of Tectonics and Applied Geology, Faculty of Geology & Geoenvironment, National and Kapodistrian University of Athens, Athens, Greece; soukis@geol.uoa.gr
* Correspondence: voudouris@geol.uoa.gr (E.G.); manosgalanos@gmail.com (P.V.); Tel.: +30-210-7274129

Abstract: Vein-type Pb-Ni-Bi-Au-Ag mineralization at Clemence mine in Kamariza and the Km 3 locality in the Lavrion area was synchronous with the intrusion of a Miocene granodiorite body and related felsic and mafic dykes and sills within marbles and schists that constitute the footwall of the Western Cycladic Detachment System. The Ni-Bi-Au association at Clemence mine consists of initial deposition of pyrite and arsenopyrite followed by an intergrowth of native gold-bismuthinite and oscillatory zoned gersdorffite. Oscillatory zoning in gersdorffite is related to variable As, Ni and Fe contents, indicating fluctuation of arsenic and sulfur fugacity in the hydrothermal fluid. A late evolution towards higher sulfur fugacity in the mineralization is evident by the deposition of chalcopyrite, tennantite, enargite and galena rimming gersdorffite. At the Km 3 locality, the observed Ni sulfides and sulfarsenides, vaesite, millerite, ullmannite and polydymite, are enclosed in gersdorffite and/or galena. The gersdorffite is homogenous and contain less Fe (up to 2 wt %) than that from the Clemence mine (up to 9 wt %). Bulk analyses for Clemence ore reveal Au and Ag grades exceeding both 100 g/t, Pb and Zn > 1 wt %, Ni up to 9700 ppm, Co up to 118 ppm, Sn > 100 ppm and Bi > 2000 ppm. The Km 3 mineralization is enriched in Mo (up to 36 ppm), Ni (>1 wt %) and Co (up to 1290 ppm). Despite local variations, both districts are characterized by a common fluid evolution similar to the broad Lavrion area.

Keywords: nickel sulfides-sulfarsenides; bismuth; gold; oscillatory zoning; Lavrion; Greece

1. Introduction

The Lavrion district in Greece is part of the Attic-Cycladic metamorphic core complex, and contains a variety of ore types including porphyry Mo-W, skarn Fe-Cu-Bi-Te, carbonate-replacement Pb-Zn-Cu-Ag ± Au-Bi and vein-type Pb-As-Sb-Ag and Pb-Ni-Bi-Au [1–7]. Mineralization was synchronous with the intrusion of a late Miocene granodiorite body in the footwall marbles and schists of the Western Cycladic Detachment System and related felsic dykes and sills, which locally cross-cut the detachment and intrude also into the hanging wall. Nickel- (and cobalt-) bearing metallic minerals have been described from several sites in the Lavrion deposit, as for example from

Kamariza, Plaka and Km 3 subdistricts. Gersdorffite, rammelsbergite and nickeline have been described from Km 3 site by Marinos and Petraschek [1], Katerinopoulos and Zissimopoulou [8], Rieck [9] and safflorite by Rieck [10]. Gersdorffite related to sulfides and fluorite has been found along the detachment fault in Villia and in chimneys from Jean Baptiste mine (Kamariza) [7]. Kolitsch et al. [6] described the following Ni and Co minerals at Plaka (adit No. 145): cattierite, cobaltite, pentlandite, polydymite, siegenite, ullmannite and violarite. Polydymite, ullmannite, vaesite and violarite were detected at Km 3 locality within galena-nickelskutterudite-gersdorffite assemblages. Vaesite and violarite were also detected in the Jean Baptiste mine (Kamariza). Gersdorffite associated with gold was described by Voudouris et al. [4] from Clemence mine, Kamariza area. The aim of the present study is to evaluate the primary mineralogical and chemical characteristics of the Clemence mine and the Km 3 locality and to obtain preliminary information of their possible genetic relations with the intrusive bodies.

2. Materials and Methods

Samples were collected from the underground Clemence mine and from the Km 3 locality. Forty-three thin and polished sections of host-rocks and the sulfide mineralization were studied by optical microscopy and a JEOL JSM 5600 scanning electron microscope, equipped with back-scattered imaging capabilities, at the Department of Mineralogy and Petrology, University of Athens. The chemical composition of sulfides, sulfosalts and native elements was determined with a Cameca-SX 100 wavelength-dispersive electron microprobe at the Department of Mineralogy and Petrology, University of Hamburg, Germany. Operating conditions were: 20 kV and 20 nA, with a beam diameter <1 μm. The following X-ray lines were used: AgLα, AsLα, AuMα, BiMβ, CuKα, FeKα, HgMα, PbMα, SKα, SbLα, SeLα, TeLα, and ZnKα. Pure elements (for Ag, Au, Bi, Se, Te), pyrite and chalcopyrite (for Fe, Cu and S), galena (for Pb), sphalerite (for Zn), HgS (for Hg), Sb_2S_3 (for Sb) and synthetic GaAs (for As) were used as standards. Mineralized samples were analyzed for their trace element content by 1:1:1 Aqua Regia digestion with Ultratrace ICP-MS analyses at ACME analytical laboratories (Vancouver, BC, Canada).

3. Geology

The Lavrion district belongs to the Attic-Cycladic Crystalline Belt, which is characterized by a Late Cretaceous-Eocene deformation and eclogite/blueschist-facies metamorphism, followed by Late Oligocene to Miocene post-orogenic extension in the back-arc region of the Aegean continental crust. The latter resulted in a greenschist- to amphibolite-facies overprint of the high-pressure rocks, formation of several metamorphic core complexes and exhumation to the surface [11,12]. The footwall Kamariza Unit composed of a sequence of Triassic-Early Jurassic rocks metamorphosed to blueschist facies and retrogressed to greenschist-amphibolite facies, consists of a Lower marble, the Kamariza schists (with minor marble intercalations), and an Upper ultramylonitic marble formation [1,13]. The Intermediate Tectonic Unit also referred as the Lavrion or Cycladic Blueschist Unit, comprises a phyllitic nappe of Late Cretaceous age [1,13,14]. It consists of a volcano-sedimentary formation (schist, marble, quartzite), with mafic meta-ophiolite blocks, and marble intercalations [13,15,16]. The Upper Unit is represented in the Lavrion area by late Jurassic red cherts and a non-metamorphosed limestone of late Cretaceous age [16,17].

The tectonic contacts between Upper, Intermediate and Kamariza units are low-angle normal faults that constitute the Western Cycladic detachment system (Figure 1) [18,19]. A late Miocene I-type granodiorite intrusion is exposed at Plaka (Figure 1), and its intrusion was synchronous with the last stages of the extensional detachment faulting [7,20,21]. Several occurrences of granites and granodiorite porphyry laccoliths, pipes, dykes and sills are exposed throughout the Lavrion district [1,7,14,21]. Carbonate-sericite altered microgranodiorite dykes and sills at Kamariza (e.g., Serpieri mine) are crosscut by porphyry-style quartz-sericite-calcite stockworks hosting sulfide mineralization including pyrrhotite, arsenopyrite, pyrite and galena (Figures 2a and 3a). In addition, east-west trending andesitic dykes crosscut the lower marble and the Kamariza schists in the Kamariza area. They are equigranular rocks consisting of plagioclase and biotite with interstitial

quartz. The dykes are propylitically altered (Figure 2b), whereas adjacent to the orebodies they are pervasively altered to quartz-sericite ± carbonates and contain disseminated or vein sulfides. According to Marinos and Petrascheck [1], the largest dykes appear north of "Serpieri 1" shaft, between the "Serpieri 1", "Hilarion 1" shafts, and south of the Hilarion orebody (Figure 1b).

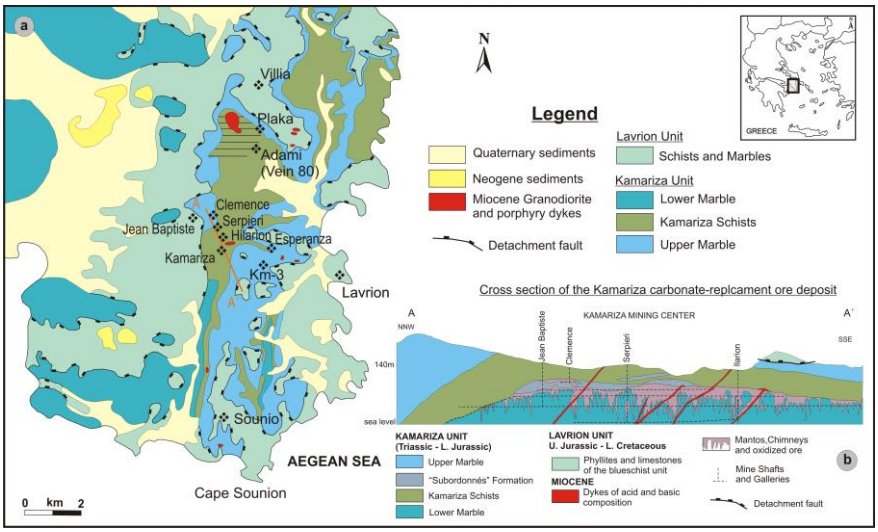

Figure 1. Simplified geological map of the Lavrion ore district (modified after Marinos and Petraschek [1]; (**b**) cross-section A–A′ of the Kamariza deposit (modified after Marinos and Petraschek [1]).

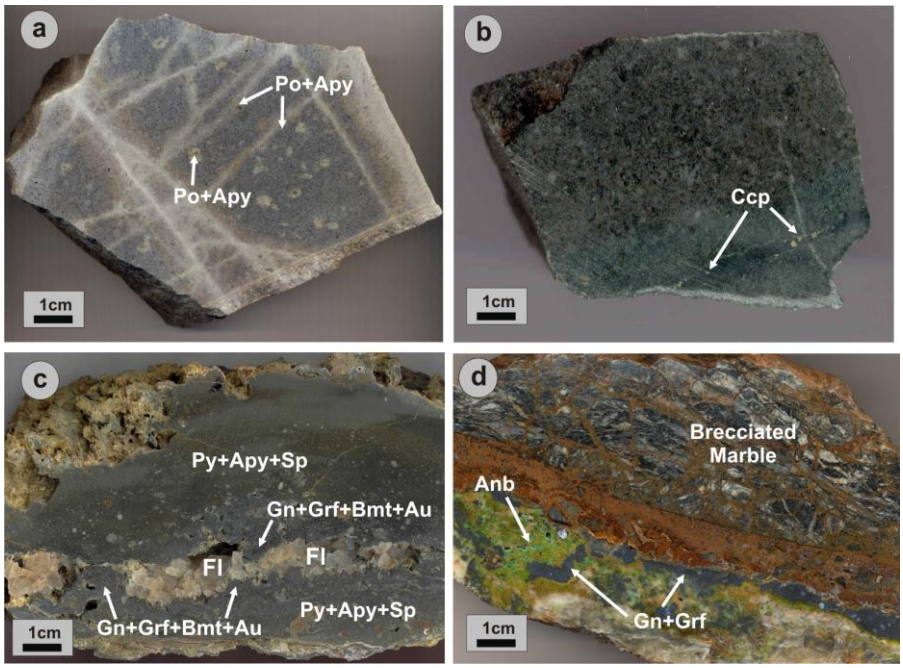

Figure 2. Hand specimens of granitoids and Ni-bearing ores at Lavrion area. (**a**) Carbonate-sericite-quartz veinlets with pyrrhotite (Po) and arsenopyrite (Apy) crosscutting a felsic sill at Serpieri Mine; (**b**) propylitic altered andesitic dyke from Jean Baptiste Mine; (**c**) banded vein-style mineralization from Clemence Mine, consisting of initial deposition of pyrite (Py) + arsenopyrite (Apy) + sphalerite (Sp), followed by the deposition of galena (Gn) + gersdorffite (Grf) + bismuthinite (Bmt) + gold (Au) and finally the deposition of fluorite (Fl); (**d**) Brecciated marble cemented by galena (Gn) + gersdorffite (Grf) mineralization. The Ni-arsenate annabergite (Anb) is a supergene alteration product of gersdorffite.

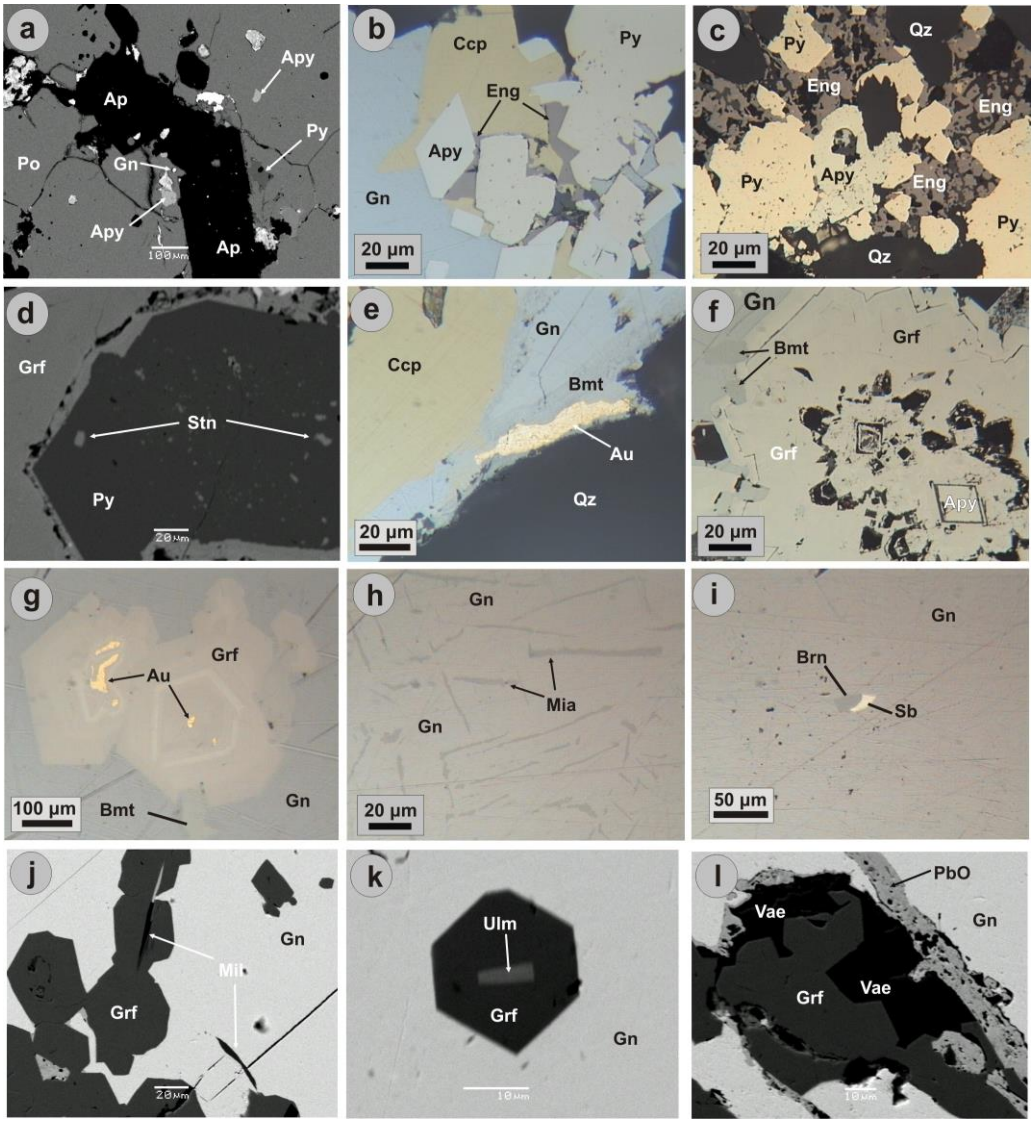

Figure 3. Photomicrographs demonstrating ore paragenesis in the Serpieri, Clemence and Km 3 areas. (**a**) Pyrrhotite (Po) including arsenopyrite (Apy), pyrite (Py) and galena (Gn). Fluorapatite (Ap) is also present. Felsic dyke from Serpieri area; (**b**) pyrite and arsenopyrite are followed by chalcopyrite (Ccp), enargite (Eng) and then by galena (CLM2, reflected light–plain polarized); (**c**) Pyrite and arsenopyrite rimmed by enargite (CLM6a, reflected light–plain polarized); (**d**) Pyrite including stannite (Stn) is surrounded by gersdorffite (Grf) (CLM6a, scanning electron microscope-back scattered electron image); (**e**) chalcopyrite postdated by galena including bismuthinite (Bmt) and native gold (Au). Quartz (Qz) is gangue mineral (CLM6, reflected light–plain polarized); (**f**) arsenopyrite rimmed by gersdorffite, the later surrounded by bismuthinite and galena (CLM6b, reflected light–plain polarized); (**g**) oscillatory zoned gersdorffite including native gold and bismuthinite is surrounded by galena (CLM6b, reflected light–plain polarized); (**h**) miargyrite (Mia) as exsolution lamellae within galena (CLM4a, reflected light–plain polarized); (**i**) bournonite (Brn) and native antimony (Sb) included in galena (CLM6a, reflected light–plain polarized); (**j**) millerite (Mil) needles included in both gersdorffite and galena ('km 3', scanning electron microscope-back scattered electron image); **k** Ullmannite (Ulm) enclosed in gersdorffite Km 3 locality, scanning electron microscope-back scattered electron image); **l** gersdorffite surrounded by vaesite (Vae), enclosed in galena (PbS).

4. Mineralization

The nickeliferous assemblage from Clemence mine is a vein-type mineralization, which is developed at the contact between marbles and schists of the Kamariza unit [4]. The mineralization also replaces marbles, where it forms extensive manto and chimney bodies. The mineralization in the Clemence vein is characterized by open space filling and mineralogical zonation. Pyrite, arsenopyrite and sphalerite dominate at the outer parts of the vein, whereas galena and fluorite at the vein center (Figure 2c). Paragenetic relationships in the vein suggest initial deposition of pyrite, arsenopyrite, stannite and Fe-rich sphalerite, followed by gersdorffite, bismuthinite and native gold, then by chalcopyrite, tennantite/tetrahedrite, bournonite, enargite and Fe-poor sphalerite, and finally by galena containing exsolved grains and inclusions of semseyite, boulangerite, native antimony, Ag-rich tetrahedrite, stephanite and miargyrite. Quartz is the main gangue mineral in the early stage of ore deposition followed by fluorite which accompanies galena. In Km 3 locality, the nickeliferous assemblage is associated with veins of calcite, dolomite and galena crosscutting brecciated upper marble of the Kamariza Unit (Figure 2d).

5. Results

5.1. Bulk Ore Geochemistry

Bulk ore analyses of Clemence ore reveal Au and Ag grades exceeding 100 g/t, Pb and Zn > 1 wt %, Ni up to 9700 ppm, Co up to 118 ppm, Sn > 100 ppm and Bi > 2000 ppm. Mineralization at Km 3 locality is enriched in Mo (up to 36 ppm), As and Ni (both >1 wt %), Co (up to 1290 ppm), whereas other elements occur in lesser amounts: Te (up to 2 ppm), Sn (up to 8.5 ppm), Bi (up to 1.3 ppm). Preliminay data on sericite altered dykes and sills indicate enrichment in Ni (up to 220 ppm), Cu (up to 175 ppm), As (up to 510 ppm), Mo (up to 6 ppm) and Pb (up to 830 ppm).

Table 1. Trace element content (in ppm) of mineralization at Clemence (CLM series) and Km 3 locality (Km3 series). Au and Hg in ppb. Bd: below detection limit.

	CLM1	CLM2	CLM3	CLM4	CLM6	CLM6B	Km3-1	Km3-2	Km3-3
Mo	0.26	0.25	0.11	1.90	0.31	0.26	4.31	35.82	11.71
Cu	5869	3485	323.4	45.06	2503	>10,000	932.8	45.22	88.93
Au	37.3	104.9	38.3	bd	>100,000	3798	78.2	16.4	75.4
Ag	>100	>100	>100	7.97	>100	>100	>100	>100	>100
Pb	>10,000	>10,000	>10,000	1441	>10,000	>10,000	>10,000	>10,000	>10,000
Zn	536.4	1129	>10,000	323.5	326.1	>10,000	4195	1591	863.7
As	>10,000	>10,000	4952	1338	>10,000	7983	>10,000	>10,000	>10,000
Sb	>2000	>2000	>2000	1554	61.98	>2000	>2000	>2000	>2000
Ni	3.1	11.6	1.1	8.9	9686	388.3	>10,000	>10,000	>10,000
Co	14.7	42.7	83.9	92.2	118.3	80.4	207.4	175.3	231
Te	1.63	1.48	1.51	0.03	1.26	1.34	1.73	2.10	2.25
Sn	28.4	27.0	25.1	0.9	16.4	>100	8.3	5.7	8.1
Bi	93.90	85.20	12.37	0.74	>2000	133.2	1.29	0.81	1.18
Hg	3529	379	1246	<5	1260	bd	2122	388	670

5.2. Ore Mineralogy

Previous work by Voudouris et al. [4] reported in detail the mineralogy and mineral-chemistry of metallic minerals from Clemence mine. Additional information is given here: in summary, pyrite has Co and Ni contents below detection limits. Pyrite includes small grains of stannite (Cu_2FeSnS_4) (Figure 3d). Arsenopyrite contains 41.1 to 43.15 wt % As which corresponds to 29.9–31.06 at % As. Early sphalerite is Fe-rich (up to 24.7 mole % FeS) and associated with arsenopyrite, whereas late sphalerite is Fe-poor (2.9 mole % FeS) and associated with the Cu-As bearing association including chalcopyrite-tennantite and enargite. Galena includes gersdorffite, semseyite, bismuthinite,

bournonite, native antimony and native gold (Figure 3). It also contains exsolved grains of boulangerite, Ag-rich tetrahedrite, stephanite (Ag_5SbS_4) and miargyrite ($AgSbS_2$) (Figure 3h). Bismuthinite is included in gersdorffite and galena (Figure 3e to g). Native gold usually forms up to 150 μm grains enclosed in gersdorffite, but can also be found as intergrowths with bismuthinite and/or as isolated grains, enclosed in galena (Figure 3e,g). It contains 11.50 to 18.56 wt % Ag [2]. Gersdorffite occurs as zoned idiomorphic crystals enclosed in galena and rimming pyrite and arsenopyrite (Figure 3d,f). It displays oscillatory zoning with respect to its Fe, Ni and As contents, varying from ~1.5 to 9 wt %, ~24 to 32 wt % and 47 to 60 wt %, respectively (Table 2, Figures 4 and 5). The Clemence gersdorffite contains up to 0.2 wt % Se substituting for sulfur in the structure. At the Km 3 locality, gersdorffite contains ~0.5–2 wt % Fe, 46–48 wt % As and ~31–34 wt % Ni (Table 2). Millerite (NiS) is found in association with gersdorffite, as small inclusions or as euhedral needle-shaped crystals enveloped by galena (Figure 3j). Ullmannite, Ni(Sb,As)S, occurs as inclusions in gersdorffite (Figure 3k). Vaesite (NiS_2) is rimming gersdorffite (Figure 3l). Cobalt (up to 0.35 wt %) substitutes for Ni in vaesite and millerite (Table 2).

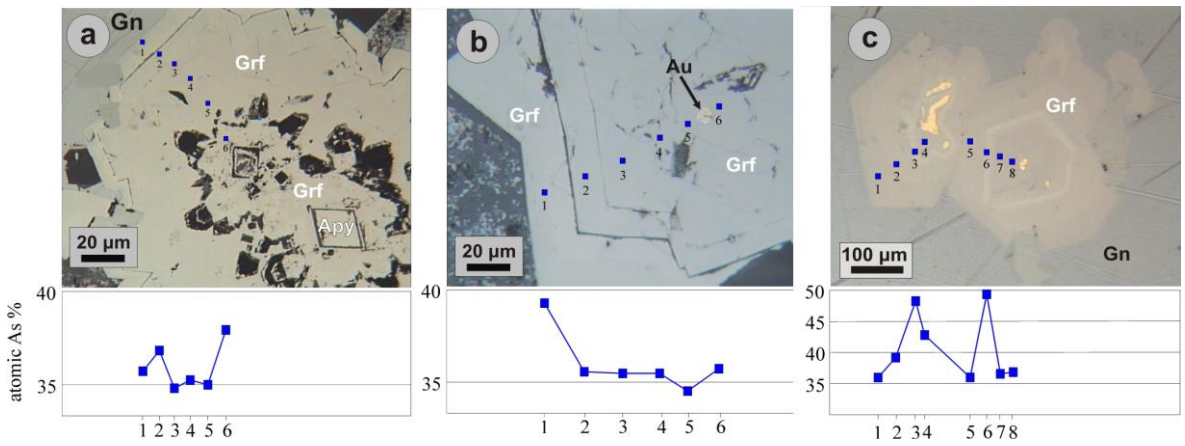

Figure 4. EMPA line scans of As distribution along traverses in gersdorffite.

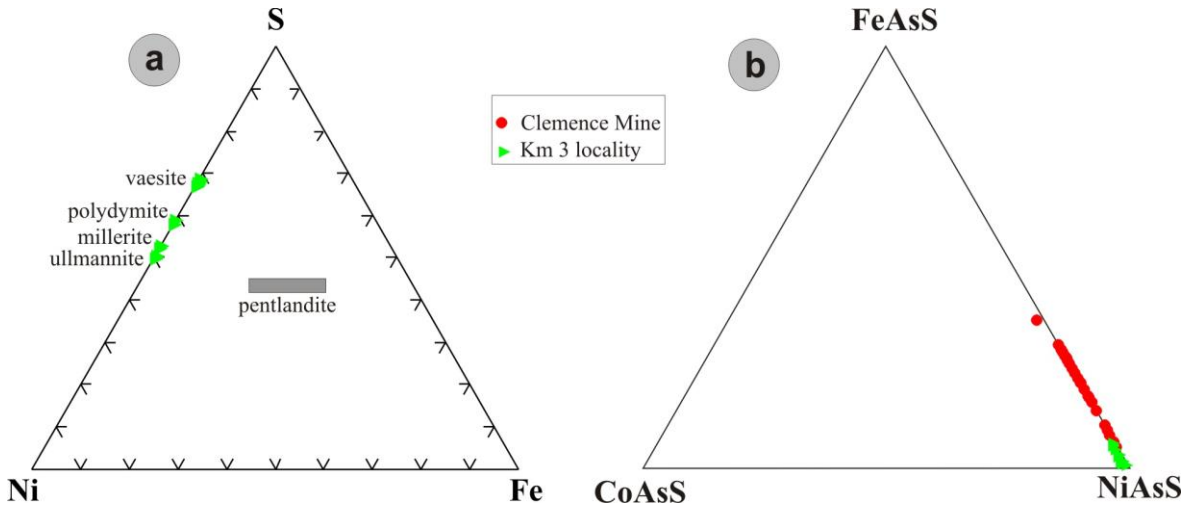

Figure 5. Chemical variation of Ni sulfides/sulfarsenides from Lavrion as a function of ternary plots in terms of (**a**) Ni, Fe, S and (**b**) Ni, Fe, Co.

Table 2. Representative electron microprobe analyses and atomic proportions of gersdorffite (1–8: Clemence Mine; 9, 10: Km 3 locality), vaesite (11, 12), millerite (13, 14); polydymite (15, 16); ullmannite 17, 18). bd: below detection limit, na: not analyzed.

	1	**2**	**3**	**4**	**5**	**6**	**7**	**8**	**9**	**10**	**11**	**12**	**13**	**14**	**15**	**16**	**17**	**18**
Ni	24.12	26.81	32.04	28.67	25.00	27.59	25.04	25.22	34.55	32.65	46.19	45.93	63.18	62.48	56.42	56.67	28.00	27.71
Fe	9.10	7.59	2.23	5.70	8.06	4.46	5.54	5.40	0.49	1.63	0.37	0.05	0.54	0.20	0.16	0.38	0.02	0.11
Co	bd	bd	bd	d	bd	bd	bd	bd	0.13	bd	0.18	0.35	0.06	0.26	bd	bd	bd	bd
Au	0.12	bd	0.07	0.08	0.06	0.25	0.29	0.29	na	na	na	na	Na	na	na	na	na	na
As	50.12	47.55	46.26	47.84	51.61	54.07	58.96	59.95	46.99	47.55	0.97	0.09	0.45	0.16	bd	bd	8.41	8.88
Sb	0.08	bd	0.78	0.10	bd	0.13	0.04	0.02	na	na	na	na	na	na	bd	bd	47.93	46.72
Bi	bd	bd	0.18	bd	bd	0.05	bd	bd	na	na	na	na	na	na	na	na	na	na
S	16.48	18.40	18.46	18.06	15.66	13.22	10.21	9.51	18.71	19.21	52.65	53.60	36.38	36.32	43.47	42.58	15.24	15.15
Se	0.16	0.17	0.19	0.15	0.14	0.20	0.20	0.18	na	na	na	na	na	na	na	na	na	na
Total	100.18	100.54	100.26	100.64	100.59	100.01	100.34	100.60	100.88	100.82	100.36	100.02	100.61	99.42	99.97	99.40	101.11	98.84
Atoms	3	3	3	3	3	3	3	3	3	3	3	3	2	2	7	7	3	3
Ni	0.700	0.759	0.915	0.816	0.730	0.835	0.782	0.792	0.975	0.918	0.962	0.955	0.967	0.963	2.902	2.943	0.977	0.977
Fe	0.278	0.226	0.067	0.170	0.247	0.142	0.182	0.178	0.016	0.048	0.008	0.001	0.008	0.003	0.009	0.021	0.000	0.000
Co	0.000	0.000	0.000	0.000	0.000	0.000	Bd	0.000	0.003	0.000	0.003	0.002	0.001	0.004	0.000	0.000	0.000	0.000
Au	0.001	0.000	0.001	0.001	0.001	0.002	0.003	0.003	-	-	-	-	-	-	-	-	-	-
As	1.140	1.056	1.035	1.067	1.181	1.282	1.443	1.475	1.039	1.048	0.016	0.002	0.006	0.001	0.000	0.000	0.230	0.245
Sb	0.001	0.000	0.011	0.001	0.000	0.002	0.001	0.000	-	-	-	-	-	-	0.000	0.000	0.806	0.796
Bi	0.000	0.000	0.001	0.000	0.000	0.000	0.000	0.000	-	-	-	-	-	-	-	-	-	-
S	0.876	0.955	0.965	0.941	0.837	0.732	0.584	0.547	0.967	0.989	2.009	2.037	1.018	1.027	4.094	4.048	0.973	0.996
Se	0.003	0.004	0.004	0.003	0.003	0.004	0.005	0.004	-	-	-	-	-	-	-	-	-	-

3. Discussion

The Ni-Bi-Au (e.g., gersdorffite-bismuthinite-native gold) association described from Clemence mine at Lavrion is uncommon, and its genesis is still a matter of further research. A magmatic contribution for metals has been proposed by Voudouris et al. [4] and Bonsall et al. [5], mainly based on the close spatial relationship of the deposits with several dykes and sills of granodioritic to andesitic composition in Kamariza. A genetic relation between nickel sulfides and sulfarsenides, native bismuth, bismuthinite, pyrrhotite and precious metals (Au, Ag) with granitoid intrusions has been reported from several ore deposits as for examples at the Fe-W Ulsan mine in S. Korea [22], Cradock in South Africa [23] and Erzgebirge, Germany [24]. For the multi-stage Ag-Bi-Co-Ni-U and Cu-Bi vein mineralization at Wittichen, Schwarzwald, SW Germany, which consists of Ni sulfarsenides, native Bi and various Bi sulfosalts, Staude et al. [25] suggested a granitic source for the occurrence of Bi in all stages and leaching from the host rock (redbeds) of some ore-forming elements, e.g., Ag, Co and Ni at temperatures from around 300 °C to <100 °C. A remobilization/leaching of Co, Ni, Fe, and As from basic/ultrabasic wallrocks has been favored for Bou Azzer, Morocco [26] and Cobalt/Ontario Canada [27]. However, at Bou Azzer, where no Bi-bearing minerals were reported, acidic magmatic fluids under moderately reducing conditions at high fluid/rock ratios leached the elements Co, Ni, Fe, and As from serpentinites [26]. Similarly, the likely source of nickel and gold in the Ni-Sb-Ag-Au association with ullmannite, allargentum, Au-rich silver and Au-bearing dyscrasite from the Kutná Hora Pb-Zn-Ag ore district (Czech Republic), was the serpentinized ultrabasic bodies, cut by the "silver" lodes in the south of the ore district [28]. The scenario of remobilization/leaching of metals from previous mineralization and/or host rocks, through the late involvement of non-magmatic, surface-derived fluids in the ore system was recently favored by Scheffer et al. [29], and already discussed by Leleu et al. [30] and Morin and Photiades [31] for the formation of the Pb-Zn-Ag breccia-style mineralization.

Oscillatory zoning is common in sulfides (e.g., pyrite, arsenopyrite, sphalerite, molybdenite and fahlores; Plotinskaya et al. [32], Deditius et al. [33], Grabezhev and Voudouris [34]). Oscillatory zoning in gersdorffite has been reported from the San Juan de Plan deposit in Spain [35], the high-grade Ni-Co-Fe-As hydrothermal vein ores from Dobšiná (Slovakia) [36], and from Pb(Ag)-Zn deposits within the Rogozna ore field, Serbo-Macedonian metallogenic province [37].

The variations in the As-, Ni- and Fe-contents in individual micro-zones observed within the oscillatory growth zones of Clemence gersdorffite suggest physical or chemical fluctuations within the bulk system and disequilibirium as stated by Shore and Fowler [38]. Changes in the hydrothermal system, such as varying fluid composition, or temperature, led to the gersdorffite zoning at Clemence deposit. Zonation in gersdorffites is attributed to intense fluctuation of arsenic fugacity and activities of Ni and Fe in the hydrothermal fluid.

Previous work by Voudouris et al. [4] suggested that the association between bismuthinite and native gold in the gold-bearing galena ores within the Clemence deposit may have been caused by the sulfidation of maldonite in response to an increase in fS_2 and that the presence of sulfarsenide minerals associated with native gold and bismuthinite in the Clemence deposit also suggests reduced hydrothermal fluids. If this was the case, maldonite should be part of a very early low-sulfidation and strongly reduced assemblage in Kamariza, in the stability field of pyrrhotite, arsenopyrite and/or löllingite (all three phases are present in Kamariza ore). Maldonite was not observed during this study; its presence in Lavrion ore is reported in association with native bismuth and native gold by Rieck [8,39]. However, Solomos et al. [3] argued for a contemporaneous deposition of chalcopyrite with bismuthinite, native bismuth and maldonite (which was later decomposed to native gold and native bismuth) for oxidized Au-Bi ores at Hilarion mine in Kamariza. Native gold also occurs as isolated grains within galena and without any contact to bismuthinite, thus suggesting that the hydrothermal fluids were probably at the boundary Au + Bi_2S_3/Au_2Bi during gold deposition.

The arsenic content of arsenopyrite in equilibrium with pyrite analyzed in this study is identical to that reported by Skarpelis [7], who estimated a variation in fS_2 values between $10^{-7.1}$ and $10^{-10.3}$ (for temperatures of 300 to 400 °C) based on the geothermometers of Kretschmar and Scott [40] and Sharp et al. [41]. Fluid inclusions in fluorite from the Clemence deposit, associated with galena,

homogenized between 233 and 275 °C [4]. Accordingly, a path of decreasing temperature (from about 400 to 200 °C), under generally increasing fS_2 conditions, as indicated also by a decrease of the Fe content of sphalerite from about 25 to 3 mole % FeS, has been suggested for the mineralization at Clemence by Voudouris et al. [4]. On the contrary, at the Km 3 locality, deposition of Ni sulfides is followed by formation of homogeneous gersdorffite, indicating increasing trends for the As content and decreasing Ni activities in the hydrothermal fluid. Late galena associated with fluorite rims gersdorffite in both districts demonstrating a common fluid evolution along the West Cycladic detachment system in the broad Lavrion area.

Author Contributions: P.V., B.R. and U.K. collected the studied samples. E.G. and P.V., assisted by C.M. and S.Z. evaluated the mineralogical data. V.M. and K.S. evaluated the geochemical and structural data respectively. E.G. and P.V. wrote the manuscript.

Acknowledgments: The authors would like to thank Evangelos Michailidis and Stefanie Heidrich for their kind help on microanalyses in the National and Kapodistrian University of Athens and Institute of Mineralogy-Petrology, University of Hamburg, respectively. Two anonymous reviewers are especially thanked for their constructive comments that greatly improved the manuscript.

Conflicts of Interest: The authors declare no conflict of interest.

References

1. Marinos, G.; Petrascheck, W.E. Geological and geophysical research. *Inst. Geol. Subsurf. Res.* **1956**.
2. Voudouris, P.; Economou-Eliopoulos, M. Mineralogy and chemistry of Cu-rich ores from the Kamariza carbonate-hosted deposit (Lavrion), Greece. In *Mineral Exploration and Sustainable Development*; Millpress: Rotterdam, The Netherlands, 2003; pp. 499–502.
3. Solomos, C.; Voudouris, P.; Katerinopoulos, A. Mineralogical studies of bismuth-gold-antimony mineralization at the area of Kamariza, Lavrion. *Bull. Geol. Soc. Greece* **2004**, *36*, 387–396. (In Greek with English abstract)
4. Voudouris, P.; Melfos, P.; Spry, P.G.; Bonsall, T.A.; Tarkian, M.; Solomos, C. Carbonate-replacement Pb-Zn-Ag ± Au mineralization in the Kamariza area, Lavrion, Greece: Mineralogy and thermochemical conditions of formation. *Mineral. Petrol.* **2008**, *94*, 85–106.
5. Bonsall, T.A.; Spry, P.G.; Voudouris, P.; Seymour, K.S.; Tombros, S.; Melfos, V. The geochemistry of carbonate-replacement Pb-Zn-Ag mineralization in the Lavrion district, Attica, Greece: Fluid inclusion, stable isotope, and rare earth element studies. *Econ. Geol.* **2011**, *106*, 619–651.
6. Kolitsch, U.; Rieck, B.; Voudouris, P. Mineralogy and genesis of the Lavrion ore deposit: New insights from the study of ore and accessory minerals. *Mitt. Österr. Mineral. Ges.* **2015**, *161*, 66.
7. Skarpelis, N. The Lavrion deposit (SE Attika, Greece): Geology, mineralogy and minor elements chemistry. *Neues Jahrb. Mineral. Abh.* **2007**, *183*, 227–249.
8. Katerinopoulos, A.; Zissimopoulou, E. *Minerals of the Lavrion Mines*; The Greek Association of Mineral and Fossil Collectors: Athens, Greece, 1994; p. 304.
9. Rieck, B. Die komplette Mineralliste. *LAPIS* **1999**, *24*, 61–63.
10. Rieck, B.; Rieck, P. Silber, Arsen und Antimon: Vererzungen im Revier Plaka (Teil II). *LAPIS* **1999**, *24*, 59–60.
11. Altherr, R.; Kreuzer, H.; Wendt, I.; Lenz, H.; Wagner, G.; Keller, J.; Harre, W.; Hohndorf, A. A late Oligocene/Early Miocene high temperature belt in the Attic-Cycladic crystalline complex (SE Pelagonian, Greece). *Geol. Jahrb.* **1982**, *23*, 97–164.
12. Jolivet, L.; Brun, J.P. Cenozoic geodynamic evolution of the Aegean region. *Int. J. Earth Sci.* **2010**, *99*, 109–138.
13. Photiades, A.; Carras, N. Stratigraphy and geological structure of the Lavrion area (Attica, Greece). *Bull. Geol. Soc. Greece* **2001**, *34*, 103–109.
14. Papanikolaou, D.J.; Syskakis, D. Geometry of acid intrusives in Plaka, Laurium and relation between magmatism and deformation. *Bull. Geol. Soc. Greece* **1991**, *25*, 355–368.
15. Baltatzis, E. Contact metamorphism of a calc-silicate hornfels from Plaka area, Laurium, Greece. *Neues Jahrb. Mineral. Monatsh.* **1981**, *11*, 481–488.
16. Bassi, E.; Soukis, K.; Lekkas, S. The presence of Vari-Kirou Pira unit at Panion Hill (SE Attica, Greece). *Bull. Geol. Soc. Greece* **2004**, *36*, 1608–1617.

17. Photiades, A.; Saccani, E. Geochemistry and tectono-magmatic significance of HP/LT metaophiolites of the Attic-Cycladic zone in the Lavrion area (Attica, Greece). *Ofioliti* **2006**, *31*, 89–102.
18. Berger, A.; Schneider, D.A.; Grasemann, B.; Stöckli, D. Footwall mineralization during Late Miocene extension along the West Cycladic Detachment System, Lavrion, Greece. *Terra Nova* **2013**, *25*, 181–191.
19. Scheffer, C.; Vanderhaeghe, O.; Lanari, P.; Tarantola, A.; Ponthus, L.; Photiades, A.; France, L. Syn- to post-orogenic exhumation of metamorphic nappes: Structure and thermobarometry of the western Attic-Cycladic metamorphic complex (Lavrion, Greece). *J. Geodyn.* **2016**, *96*, 174–193.
20. Altherr, R.; Siebel, W. I-type plutonism in a continental back-arc setting: Miocene granitoids and monzonites from the central Aegean Sea, Greece. *Contrib. Mineral. Petrol*. **2002**, *143*, 397–415.
21. Skarpelis, N.; Tsikouras, B.; Pe-Piper, G. The miocene igneous rocks in the Basl unit of Lavrion (SE Attica Greece): Petrology and geodynamic implications. *Geol. Mag.* **2008**, *145*, 1–15.
22. Choi, S.G.; Youm, S.J. Compositional variation of arsenopyrite and fluid evolution at the Ulsan deposit, southeastern Korea: A low-sulfidation porphyry system. *Can. Mineral.* **2000**, *38*, 567–583.
23. Henning, A.; Van der Westhuizen, W.A.; De Bruiyn, H.; Beukes, G.J. Hydrothermal Cu-Ni-Au-Ag mineralization in a granodiorite sill north of Cradock, Republic of South Africa. *Miner. Deposita* **1997**, *32*, 410–418.
24. Seifert, T.; Sandmann, D. Metallogeny and economic potential of tungsten deposits in the Erzgebirge, Saxony/Bohemia. In Proceedings of the International Geological Congress, Oslo, Norway, 6–14 August 2008.
25. Staude, S.; Werner, W.; Mordhorst, T.; Wemmer, K.; Jacob, D.E.; Markl, G. Multi-stage Ag-Bi-Co-Ni-U and Cu-Bi vein mineralization at Wittichen, Schwarzwald, SW Germany: Geological setting, ore mineralogy, and fluid evolution. *Miner. Deposita* **2012**, *47*, 251–276.
26. Ahmed, A.H.; Arai, S.; Ikenne, M. Mineralogy and paragenesis of the Co-Ni arsenide ores of Bou Azzer, Anti-Atlas, Morocco. *Econ. Geol.* **2009**, *104*, 249–266.
27. Marshall, D.D.; Diamond, L.W.; Skippen, G.B. Silver transport and deposition at Cobalt, Ontario, Canada: Fluid inclusion evidence. *Econ. Geol.* **1993**, *88*, 837–854.
28. Pažout, R.; Šrein, V.; Korbelová, Z. An unusual Ni-Sb-Ag-Au association of ullmannite, allargentum, Au-rich silver and Au-bearing dyscrasite from Oselské pásmo "silver" Lode of Kutná Hora Pb-Zn-Ag ore district (Czech Republic). *J. Geosci.* **2017**, *62*, 247–252.
29. Scheffer, C.; Tarantola, A.; Vanderhaeghe, O.; Voudouris, P.; Rigaudier, T.; Photiades, A.; Morin, D.; Alloucherie, A. The Lavrion Pb-Zn-Fe-Cu-Ag detachment-related district (Attica, Greece): Structural control on hydrothermal flow and element transfer-deposition. *Tectonophysics* **2017**, *717*, 607–627.
30. Leleu, M.; Morikis, A.; Picot, P. Sur des minéralisations de type skarn au Laurium Leleu, M., Morikis, A., Picot, P., 1973. Sur des minéralisations de type skarn au Laurium (Grèce). *Mineral. Deposita* **1973**, *8*, 259–263.
31. Morin, D.; Photiades, A. Les techniques d'exploitation en gisements métallifèresprofonds dans l'Antiquité: Approche géologique et technologique. Les mines duLaurion (Grèce). In *Die Schätze der Erde–Natürliche Ressourcen in der Antiken Welt*; 2012; pp. 281–335.
32. Plotinskaya, O.Y.; Rusinov, V.L.; Seltmann, R. Oscillatory zoning fahlores from Au-Ag epithermal deposits. In *Goldschmidt Conference Abstracts*; 2007.
33. Deditius, A.P.; Utsunomiya, S.; Renock, D.; Ewing, R.C.; Ramana, C.V.; Becker, U.; Kesler, S.E. A proposed new form of arsenian pyrite: Composition, nanostructure and geochemical significance. *Geochim. Cosmochim. Acta* **2008**, *72*, 2919–2933.
34. Grabezhev, A.; Voudouris, P. Rhenium distribution in molybdenite from Vosnesensk porphyry Cu ± (Mo-Au) deposit (southern Urals, Russia). *Can. Mineral*. **2014**, *52*, 671–686.
35. Fanlo, I.; Subías, I.; Gervilla, F.; Paniagua, A.; García, B. The composition of Co-Ni-Fe sulfarsenides, diarsenides and triarsenides from the San Juan de Plan deposit, central Pyrenees, Spain. *Can. Mineral*. **2004**, *42*, 1221–1240.
36. Kiefer, S.; Majzlan, J.; Chovan, M.; Števko, M. Mineral compositions and phase relations of the complex sulfarsenides and arsenides from Dobšiná (Western Carpathians, Slovakia). *Ore Geol. Rev.* **2017**, *89*, 894–908.
37. Radosavljević, S.A.; Stojanović, J.N.; Vuković, N.S.; Radosavljević-Mihajlović, A.S.; Kašić, V.D. Low-temperature Ni-As-Sb-S mineralization of the Pb(Ag)-Zn deposits within the Rogozna ore field, Serbo-Macedonian Metallogenic Province: Ore mineralogy, crystal chemistry and paragenetic relationships. *Ore Geol. Rev.* **2015**, *65*, 213–227.

38. Shore, M.; Fowler, A.D. Oscillatory zoning in minerals: A common phenomenon. *Can. Mineral.* **1996**, *34*, 1111–1126.
39. Rieck, B.; Seltene Arsenate aus der Kamariza und weitere Neufunde aus Lavrion. *LAPIS* **1999**, *24*, 68–76.
40. Kretschmar, U.; Scott, S.D. Phase relations involving arsenopyrite in the system Fe-As-S and their application. *Can. Mineral.* **1976**, *14*, 364–386.
41. Sharp, Z.D.; Essene, E.J.; Kelly, W.C. A re-examination of the arsenopyrite geothermometer: Pressure considerations and applications to natural assemblages. *Can. Mineral.* **1985**, *23*, 517–534.